Brief Communication

Cell Chemical Biology

A Clickable APEX Probe for Proximity-Dependent Proteomic Profiling in Yeast

Graphical Abstract

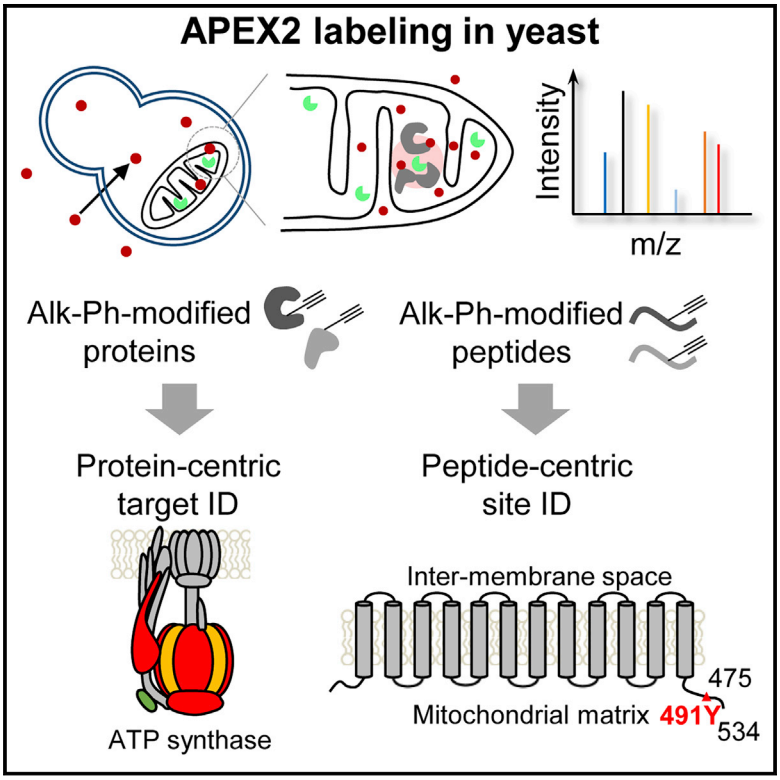

Highlights

- Clickable APEX substrate for subcellular proteomic profiling in yeast
- Improved method for identifying APEX-labeling sites
- Enabling spatially restricted transcriptome profiling in yeast

Authors

Yi Li, Caiping Tian, Keke Liu, Ying Zhou, Jing Yang, Peng Zou

Correspondence

yangjing54@hotmail.com (J.Y.), zoupeng@pku.edu.cn (P.Z.)

In Brief

By using the clickable APEX2 substrate Alk-Ph, Li et al. achieve proximity-dependent protein and RNA labeling in intact yeast cells. This new approach enables the proteomic and transcriptomic mapping of yeast mitochondrial matrix with high specificity and coverage, thus extending APEX applications to microorganisms.

Li et al., 2020, Cell Chemical Biology *27*, 1–8
July 16, 2020
https://doi.org/10.1016/j.chembiol.2020.05.006

CellPress

Please cite this article in press as: Li et al., A Clickable APEX Probe for Proximity-Dependent Proteomic Profiling in Yeast, Cell Chemical Biology (2020), https://doi.org/10.1016/j.chembiol.2020.05.006

Cell Chemical Biology

CellPress

Brief Communication

A Clickable APEX Probe for Proximity-Dependent Proteomic Profiling in Yeast

Yi Li,[1] Caiping Tian,[2] Keke Liu,[2] Ying Zhou,[1] Jing Yang,[2,*] and Peng Zou[1,3,4,*]

[1]College of Chemistry and Molecular Engineering, Synthetic and Functional Biomolecules Center, Beijing National Laboratory for Molecular Sciences, Key Laboratory of Bioorganic Chemistry and Molecular Engineering of Ministry of Education, Peking University, Beijing 100871, China

[2]State Key Laboratory of Proteomics, National Center for Protein Sciences, Beijing Proteome Research Center, Beijing Institute of Lifeomics, Beijing 102206, China

[3]Peking-Tsinghua Center for Life Sciences, PKU-IDG/McGovern Institute for Brain Research, Peking University, Beijing 100871, China

[4]Lead Contact

*Correspondence: yangjing54@hotmail.com (J.Y.), zoupeng@pku.edu.cn (P.Z.)

https://doi.org/10.1016/j.chembiol.2020.05.006

SUMMARY

The engineered ascorbate peroxidase (APEX) is a powerful tool for the proximity-dependent labeling of proteins and RNAs in live cells. Although widely use in mammalian cells, APEX applications in microorganisms have been hampered by the poor labeling efficiency of its biotin-phenol (BP) substrate. In this study, we sought to address this challenge by designing and screening a panel of alkyne-functionalized substrates. Our best probe, Alk-Ph, substantially improves APEX-labeling efficiency in intact yeast cells, as it is more cell wall-permeant than BP. Through a combination of protein-centric and peptide-centric chemoproteomic experiments, we have identified 165 proteins with a specificity of 94% in the yeast mitochondrial matrix. In addition, we have demonstrated that Alk-Ph is useful for proximity-dependent RNA labeling in yeast, thus expanding the scope of APEX-seq. We envision that this improved APEX-labeling strategy would set the stage for the large-scale mapping of spatial proteome and transcriptome in yeast.

INTRODUCTION

Eukaryotic cells are highly compartmentalized. Understanding the spatial organization of the cellular proteome is thus crucial for elucidating the molecular mechanism of cellular physiology (Beck et al., 2011; Kim and Roux, 2016). Over the past decade, proximity-dependent protein-labeling reactions, including ascorbate peroxidase (APEX) (Rhee et al., 2013)/APEX2 (Lam et al., 2015), and BioID (Choi-Rhee et al., 2004)/TurboID (Branon et al., 2018), have emerged as powerful techniques for profiling the molecular inventories of various important subcellular compartments (Kim and Roux, 2016). Among these, APEX is an engineered peroxidase that catalyzes the one-electron oxidation of biotin-conjugated phenol (BP) substrate into a phenoxyl free radical, which rapidly reacts with nearby proteins to form a covalent linkage with electron-rich amino acid side chains (Rhee et al., 2013). Due to the high reactivity and the short lifetime of phenoxyl radicals, APEX-mediated proximity labeling is characterized with fast labeling kinetics (<1 min) (Mortensen and Skibsted, 1997) and a small labeling radius (~10 nm) (Bendayan, 2001; Mayer and Bendayan, 1997). Since its invention in 2013, APEX labeling has complemented classic fractionation-based methods to provide a comprehensive proteomic map of the mitochondria (Hung et al., 2014, 2017; Rhee et al., 2013), signaling complexes (Paek et al., 2017), RNA granules (Markmiller et al., 2018), etc., in the live cell context. Notably, a majority of APEX applications are in metazoan cells, with only a few examples in microorganisms, such as yeast cells (Hwang and Espenshade, 2016; Santin et al., 2018; Singer-Krüger et al., 2020).

Yeast is a powerful model organism for studying eukaryotic cell biology (Duina et al., 2014; Pan, 2011). However, APEX labeling has not been successful in yeast due to the poor cellular permeability of its BP substrate (Hwang and Espenshade, 2016; Singer-Krüger et al., 2020). To facilitate probe penetration, the yeast cell wall had to be partially destroyed via the action of zymolase (Hwang and Espenshade, 2016) or freeze-thaw cycle (Singer-Krüger et al., 2020). We reasoned that replacing the biotin moiety with a small clickable handle, such as an alkynyl group, could improve the membrane permeability of APEX substrate. Owing to its promiscuity in substrate recognition, APEX is known to turn over alkyne-conjugated phenol (Rhee et al., 2013), a feature that motivated us to design a strategy to solve the problem of APEX labeling in yeast. As outlined in Figure 1A, following APEX-mediated labeling and cell lysis, the alkynyl handle could then be derivatized with biotin-conjugated azide using click chemistry reaction for visualization and enrichment.

Please cite this article in press as: Li et al., A Clickable APEX Probe for Proximity-Dependent Proteomic Profiling in Yeast, Cell Chemical Biology (2020), https://doi.org/10.1016/j.chembiol.2020.05.006

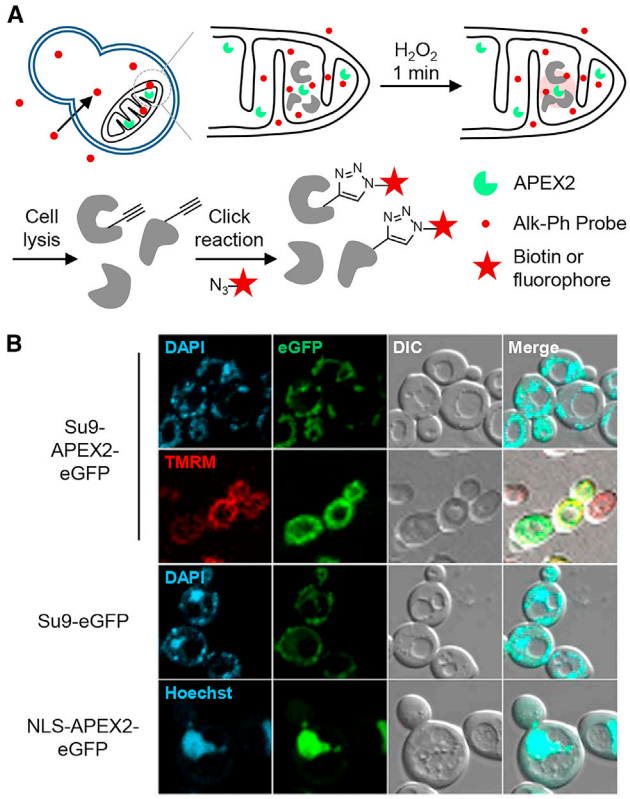

Figure 1. APEX Labeling of Yeast Subcellular Proteome

(A) Scheme of APEX-mediated labeling with Alk-Ph probe in yeast. APEX2 is genetically targeted to the mitochondrial matrix. Following Alk-Ph probe incubation, labeling reaction is triggered by the addition of 1 mM H_2O_2 and quenched after 1 min. After cell lysis, an affinity tag or a fluorophore is ligated to alkyne-modified proteins via click chemistry.

(B) Confocal fluorescence images of W303 yeast cells expressing Su9-APEX2-eGFP, Su9-eGFP, and NLS-APEX2-eGFP. Mitochondria was stained by either DAPI (Williamson and Fennell, 1979) or tetramethylrhodamine methyl ester (TMRM) and the nucleus was stained by Hoechst 33342. Scale bar, 5 μm.

RESULTS

We started by targeting APEX2 enzyme to subcellular compartments in budding yeast (tryptophan-auxotrophic W303 *Saccharomyces cerevisiae* strain) through fusion with signal peptides and proteins. We focused on the mitochondrial matrix targeting because yeast has been a favorite model for studying mitochondrial functions (Pan, 2011), yet the sub-mitochondrial localization of specific proteins could be mis-annotated even in well-established databases (Vögtle et al., 2017). For this purpose, APEX2 was fused to the pre-sequence of F_0-ATPase subunit 9 (Su9) (Westermann and Neupert, 2000) and a Flag-tagged enhanced GFP (eGFP) at its N and C termini, respectively. As a negative control, we constructed an Su9-Flag-eGFP without APEX2 fusion. For comparison, we also created a nucleus-localized APEX2 via N-terminal fusion with a nuclear localization sequence (NLS) derived from SV40 large T antigen (Kalderon et al., 1984). The correct subcellular localizations of these fusion proteins were confirmed by confocal fluorescence microscopy (Figure 1B).

We next screened a panel of alkyne-conjugated aromatic APEX2 substrates (Figure 2A) for their protein-labeling activities in intact yeast cells. These include phenol, aniline, pyridinol compounds that differ in their molecular sizes, steric hindrance, redox potentials, and bond dissociation energies. Yeast cells expressing Su9-APEX2 were incubated with each probe at 2.5 mM final concentration for half an hour, and the labeling reaction was initiated by the addition of 1 mM H_2O_2. The reaction was promptly stopped after 1 min through the addition of a cocktail of free radical quenchers, including sodium ascorbate and trolox, and a peroxidase inhibitor, sodium azide. Following cell lysis, extracted proteins were reacted with either azide-conjugated Cy5 fluorophore or azide-$(PEG)_3$-biotin for 1 h at room temperature. In-gel fluorescence imaging (Figure 2B) and western blot analysis (Figures S1A and S1B) revealed probe **1** (alkyne-phenol [Alk-Ph]) as the most reactive APEX2 substrate for labeling the yeast proteome.

We subsequently optimized the protein extraction protocol (Figures S1C–S1E), Alk-Ph probe concentration (Figures S1F–S1H), incubation time (Figures S1I–S1K), and APEX2 labeling time (Figures S1L–S1N), and compared the labeling efficiencies of Alk-Ph and BP probes in the yeast mitochondria. Whereas BP yielded negligible labeling signal, Alk-Ph labeling was substantially stronger and depended on APEX2 expression and the presence of H_2O_2 (Figure 2C). In the negative control cells expressing Su9-eGFP, we observed a weak but noticeable background Alk-Ph labeling signal in the streptavidin-horseradish peroxidase (HRP) blot (lane 3 in Figure 2C), which might be attributed to endogenous peroxidase activities in the yeast. Interestingly, we also noticed the disappearance of the anti-Flag (sequence DYKDDDDK, an epitope tag on APEX2 construct) signal on the western blot (bottom part of Figure 2C). It is likely that Alk-Ph labeling on the tyrosine residues of the FLAG tag blocks antibody recognition (Rhee et al., 2013). Due to its higher solubility in aqueous solution, the Alk-Ph probe could be supplied at a much higher concentration (>5 mM) than BP (<0.5 mM). Our probe titration data showed that APEX2-mediated Alk-Ph labeling in the yeast mitochondria is more effective at probe concentrations above 1 mM (Figure S1F). In previous work, yeast cells should be treated with high osmotic sorbitol solution to facilitate BP entry through the cell wall (Hwang and Espenshade, 2016). In contrast, our data showed that 1.2 M sorbitol treatment did not increase Alk-Ph labeling efficiency in yeast, thus confirming the good cell wall permeability of the Alk-Ph probe (Figures S2A and S2B). When APEX2 was expressed in the nucleus (NLS-APEX2) or in the secretory pathway as a fusion with the yeast a-agglutinin-binding subunit (Aga2p-APEX2), distinct subpopulations of the cellular proteome were labeled (Figures S2C–S2E). We also observed stronger Alk-Ph labeling signal than BP in another yeast strain MHY500 (Figures S2F–S2H). Taken together, the above results demonstrated the high efficiency and general applicability of APEX2-mediated protein labeling with Alk-Ph in intact yeast cells.

We applied APEX2-mediated Alk-Ph labeling to map the yeast mitochondrial matrix proteome. To quantify the level of enrichment, we designed two negative control experiments, where either the Alk-Ph probe or the APEX2 enzyme was omitted from the labeling reaction (Figure 2D). While the control omitting the probe serves to subtract the non-specific protein adsorption

Please cite this article in press as: Li et al., A Clickable APEX Probe for Proximity-Dependent Proteomic Profiling in Yeast, Cell Chemical Biology (2020), https://doi.org/10.1016/j.chembiol.2020.05.006

CellPress

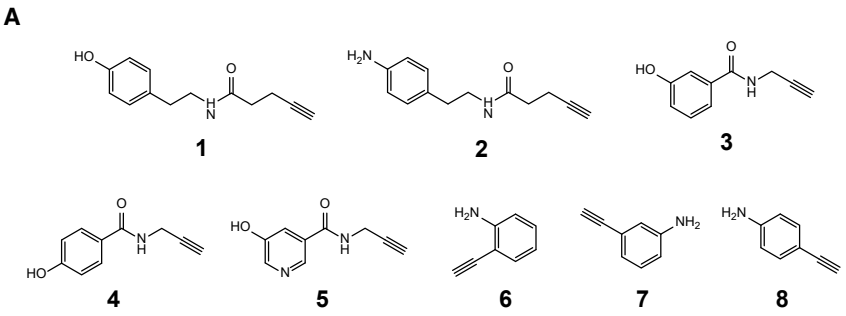

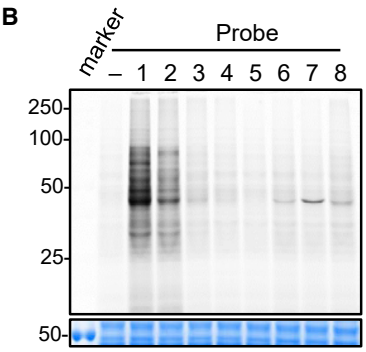

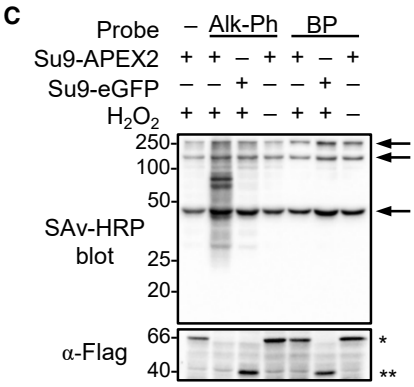

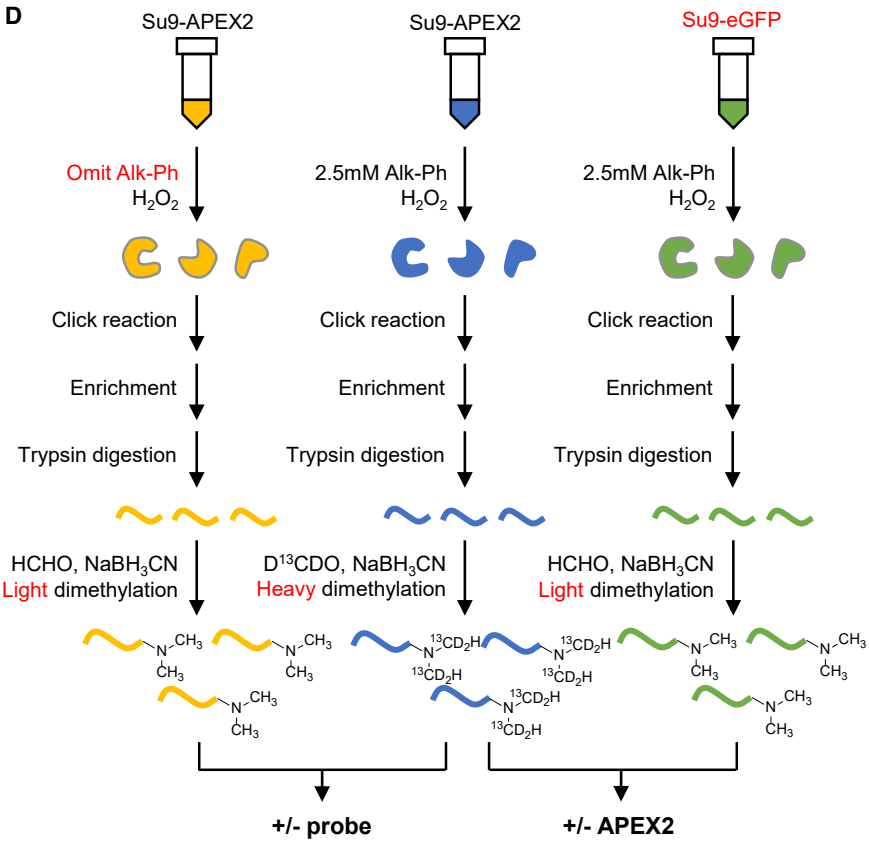

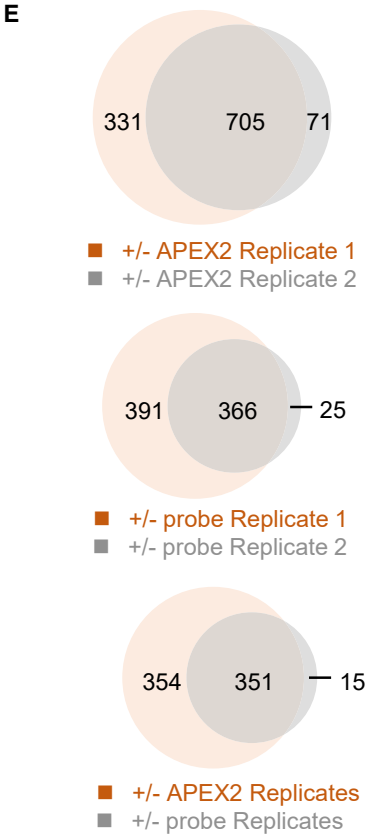

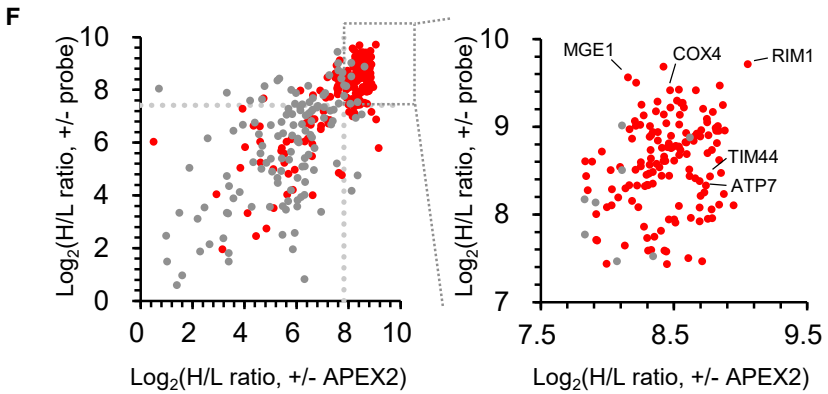

(legend on next page)

Please cite this article in press as: Li et al., A Clickable APEX Probe for Proximity-Dependent Proteomic Profiling in Yeast, Cell Chemical Biology (2020), https://doi.org/10.1016/j.chembiol.2020.05.006

background on streptavidin-coated beads, the control omitting the enzyme (using yeast cells expressing Su9-Flag-eGFP) could help remove false positives arising from the endogenous peroxidase activity in yeast, as observed earlier in the streptavidin-HRP blot (Figure 2C). For both labeling and control experiments, following cell lysis and click reaction with azide-$(PEG)_3$-biotin, labeled proteins were purified using streptavidin-coated agarose beads. The strong interactions between biotin and streptavidin allowed stringent washing of the beads with 2% SDS and 8 M urea to remove non-specific adsorption (see STAR Methods). Thereafter, enriched proteins were treated with trypsin and released from the beads in the form of digested peptides. We used a stable isotope dimethyl labeling strategy to quantitatively measure the ratio of protein abundance between samples (Figure 2D). Specifically, peptides from the labeling sample were treated with heavy isotope-labeled $D^{13}CDO$ and $NaBH_3CN$ to methylate its $–NH_2$ group, resulting in a +34.0631-Da mass shift in m/z. In contrast, peptides from each control sample were treated with HCHO and $NaBH_3CN$, leading to N-dimethylation and a mass shift of +28.0313 Da. The heavy and light samples were mixed and analyzed by liquid chromatography-tandem mass spectrometry (LC-MS/MS) for peptide identification and abundance determination, following previously established analysis protocols (Hsu et al., 2003; Hung et al., 2016).

A total of 705 and 366 proteins were identified across two biological replicate experiments of ±APEX2 quantitative MS analysis and two biological replicate experiments of ±probe quantitative MS analysis, respectively (Figure 2E; Table S1). The H/L (heavy to light) ratio cutoff was determined through receiver operating characteristic (ROC) analysis (Fawcett, 2006; Hung et al., 2016). We started by carefully curating a true positive list of 220 proteins, including experimentally validated mitochondrial matrix proteins (Vögtle et al., 2017) and mitochondrial ribosomal proteins (The UniProt, 2014) (Table S2). We also created a false positive list, including 66 cytoplasmic ribosomal proteins (The UniProt, 2014) and 154 proteins located at the outer mitochondrial membrane or the inter-membrane space (Vögtle et al., 2017) (Table S3). ROC analysis reveals a $\log_2$(H/L) ratio cutoff of 7.82 for ±APEX2 experiment, leading to the enrichment of 267 proteins (Figures S2I and S2J). A similar analysis with the ±probe experiments identified 209 enriched proteins above a cutoff of $\log_2(H/L) > 7.43$. Taken together, an intersection of the above two datasets yielded a list of 150 enriched proteins, including 142 proteins (95%) with previous mitochondrial annotations (Dennis et al., 2003; The UniProt, 2014) (Figures 2F and S2K; Table S1). The remaining eight proteins could be mitochondrial localized but previously mis-annonated, or they could arise from the non-specific binding to streptavidin-coated agarose beads.

While the above quantitative MS analysis has demonstrated the high spatial specificity of APEX2-mediated protein labeling with Alk-Ph in yeast, affinity purification of biotinylated proteins with beads is inevitably complicated by the non-specific protein adsorption background. An alternative strategy is to identify the Alk-Ph-modified peptides on MS, which could unambiguously assign tagged proteins/sites. To facilitate the site-specific mapping of Alk-Ph modification, we used a peptide-centric chemoproteomic workflow (Yang et al., 2015), as outlined in Figure 3A. Following APEX2 labeling, cell lysis, and tryptic digestion, peptides are clicked with an affinity tag bearing a UV-cleavable benzoinester linker (Az-UV-biotin) (Figures S3A and S3B). Biotinylated peptides are enriched by streptavidin and photo-released via UV illumination. The photo-cleavage products are then analyzed by LC-MS/MS to determine peptide sequences and Alk-Ph modification sites. Consistent with previous reports, our analysis revealed tyrosine residue as the primary site of Alk-Ph modification (Rhee et al., 2013). For example, we identified an Alk-Ph-derived modification on Y85 of yeast ATP synthase subunit H (ATP14), as demonstrated by the fully annotated MS/MS spectrum with diagnostic fragment ions specific to the modification (Figure 3B).

We have identified 56 proteins with two or more unique Alk-Ph-modified peptides in two experimental replicates, with 95% (53 out of 56) having prior mitochondrial annotations (Table S4). The majority of proteins on this list are soluble proteins, with only one exception: a multipass transmembrane protein, COX1, which is localized to the inner mitochondrial membrane (IMM) with known topology. In both replicated experiments, COX1 was consistently labeled at Y491 on the matrix side, where APEX2 was targeted (Figure S3C). Although this is the only example of identifying APEX2 labeling site on integral membrane proteins, it highlights the possibility of inferring membrane protein topology through APEX2-mediated Alk-Ph labeling, as has been previously done with the (desthiol)biotin-phenol probe (Lee et al., 2017; Udeshi et al., 2017).

The union of our peptide-ID dataset and protein-ID dataset yields a final list of 165 proteins with 94% (155 out of 165) mito-specificity, which we defined as our yeast mito-matrix proteomic dataset (Figure 3C; Table S5). Notably, our proteome possesses a much higher coverage than that achieved by previous APEX2 BP method using freeze-thaw cycle (165 versus 78

Figure 2. APEX2-Mediated Proteomic Labeling in Yeast Mitochondria with Improved Alkyne-Conjugated Substrates

(A) The chemical structure of a panel of APEX2 substrates used in this study.

(B) In-gel fluorescence image of APEX2-mediated proteomic labeling with various probes in yeast mitochondria. Alkyne-modified proteins were ligated with azide-Cy5 via click reaction. Bottom: Coomassie staining of the same gel.

(C) Streptavidin-HRP blot analysis to compare APEX2-labeling efficiency in the yeast mitochondria with Alk-Ph or BP probe. Alkyne-modified proteins were ligated with azide-$(PEG)_3$-biotin via click reaction. Molecular weight standards are shown in kDa. Arrows indicate endogenously biotinylated proteins. Bottom: α-Flag western blot showing the expression of Su9-APEX2 (*) and Su9-eGFP (**).

(D) Workflow of protein-level quantitative proteomic experiments. Stable isotope-labeled formaldehyde is used to dimethylate amino groups in the digested peptides. Negative controls are yeast cells treated in the absence of the Alk-Ph probe (-probe), or yeast cells not expressing the APEX2 enzyme (-APEX2). Duplicated experiments were performed for each condition.

(E) Venn diagrams showing the numbers of proteins identified across replicated proteomic experiments. Top: overlap between two ±APEX2 experiments. Middle: overlap between two ±probe experiments. Bottom: overlap between ±APEX2 replicates and ±probe replicates.

(F) Scatterplot showing the enrichment levels of proteins labeled with APEX2 in the yeast mitochondria. Red and gray dots represent proteins with and without mitochondrial annotations, respectively. H/L ratio cutoffs are shown as gray dashed lines. A zoom-in view is shown on the right.

Please cite this article in press as: Li et al., A Clickable APEX Probe for Proximity-Dependent Proteomic Profiling in Yeast, Cell Chemical Biology (2020), https://doi.org/10.1016/j.chembiol.2020.05.006

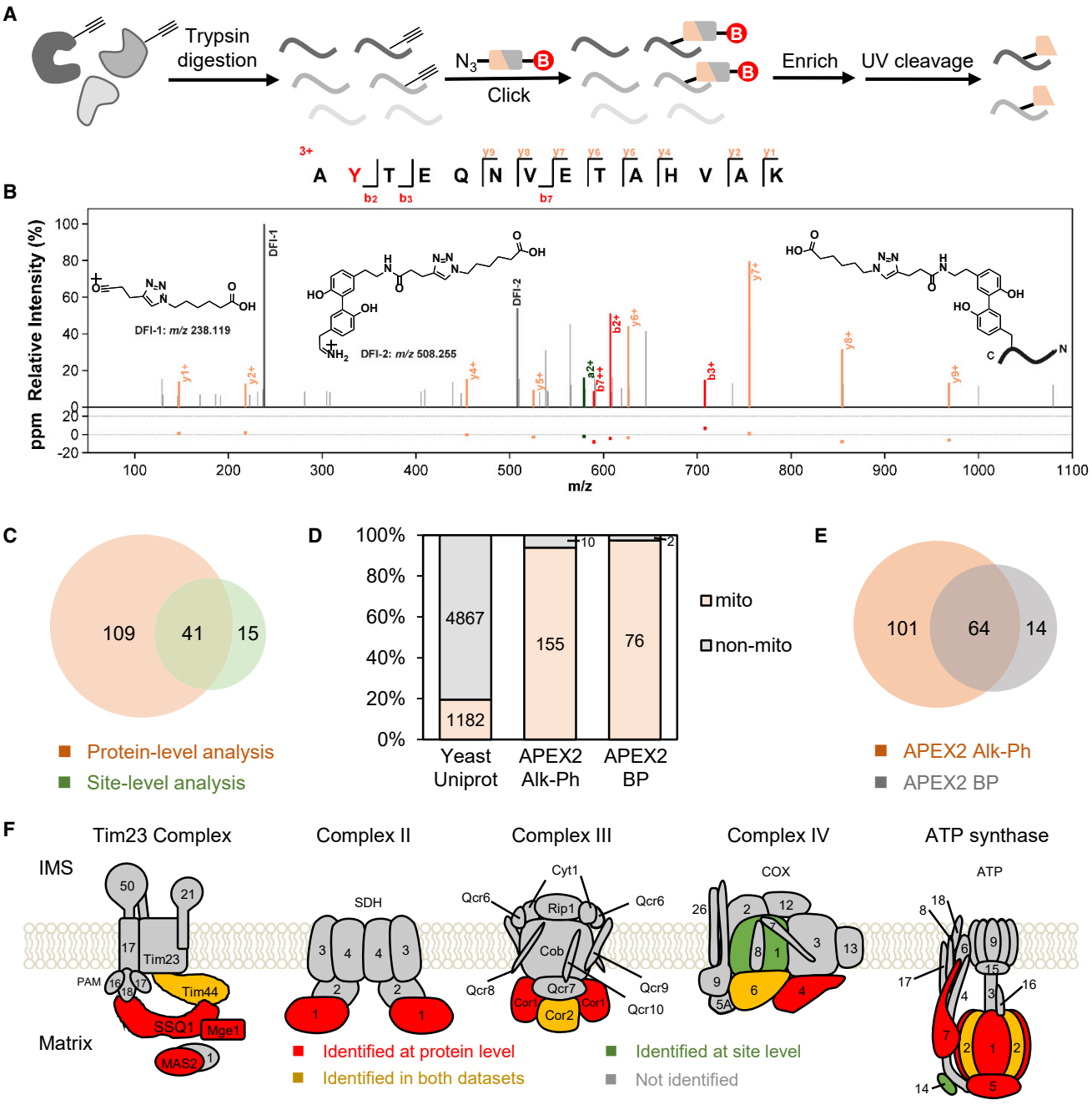

Figure 3. Identification of APEX2-Labeling Sites and Analysis of Yeast Mitochondrial Matrix Proteome

(A) Scheme of functionalizing alkyne-modified peptides with a photocleavable affinity tag (azide-UV-biotin) to assist APEX2-labeling site identification.

(B) Characteristic fragmentation of an Alk-Ph-modified peptide and its MS/MS spectrum. DFI, diagnostic fragment ions.

(C) Venn diagram showing the numbers of proteins identified in protein- and site-level analyses.

(D) Analysis of the mitochondrial specificity of APEX2 labeling. Left: proteins with prior mitochondrial annotations in the entire *S. cerevisiae* proteome (from Uniprot database). Middle: our mitochondrial matrix proteome labeled with Alk-Ph. Right: previous mitochondrial matrix proteome (Singer-Krüger et al., 2020) labeled with BP.

(E) Comparison of the APEX2-labeling coverage with Alk-Ph and BP probes.

(F) Analysis of the spatial specificity and the coverage of mitochondrial matrix labeling. Cartoons showing the subunit organization of OXPHOS complexes and the TIM/PAM proteins across the inner mitochondrial membrane (IMM). Protein subunits identified at the protein level and the site level are colored in red and green, respectively. Proteins identified in both datasets are colored in orange. IMS, inter-membrane space.

Please cite this article in press as: Li et al., A Clickable APEX Probe for Proximity-Dependent Proteomic Profiling in Yeast, Cell Chemical Biology (2020), https://doi.org/10.1016/j.chembiol.2020.05.006

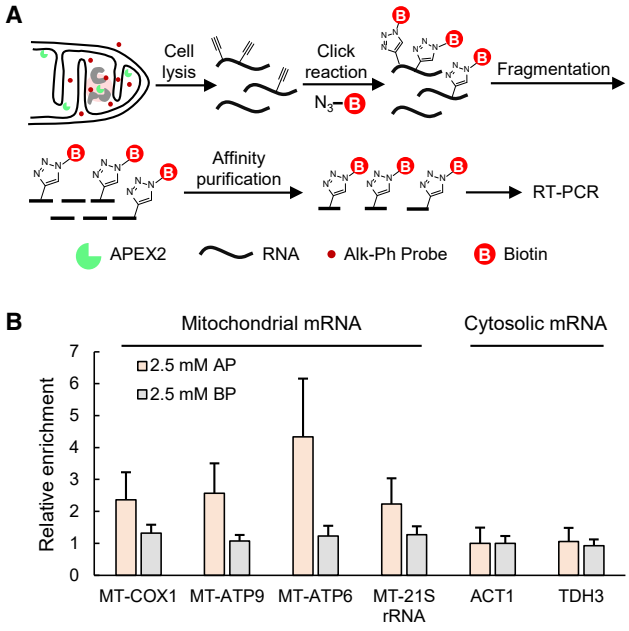

Figure 4. APEX2-Mediated Alk-Ph Labeling of the Mitochondrial Transcriptome

(A) Scheme of RNA labeling in yeast. Yeast cells expressing Su9-APEX2 were labeled with 2.5 mM Alk-Ph or BP, as previously described. Following cell lysis, alkyne-modified RNA molecules were conjugated with azide-$(PEG)_3$-biotin via click reaction, fragmented and enriched with streptavidin-coated beads. RNA abundance was quantified with real-time PCR.

(B) Real-time-PCR analysis of mitochondrial RNA enrichment (*MT-COX1*, *MT-ATP9*, *MT-ATP6*, and *MT-21S rRNA*) relative to the cytoplasmic RNA markers, *ACT1* and *THD3*. The relative enrichment levels were calculated as the ratios of $2^{-\Delta\Delta Ct}$ for each gene over that of *ACT1*, where $\Delta\Delta Ct = [Ct_{ENRICH} - Ct_{INPUT}]_{LABEL} - [Ct_{ENRICH} - Ct_{INPUT}]_{CONTROL}$ (see STAR Methods). AP, Alk-Ph probe. Error bars represent standard deviations of four technical replicates.

proteins) (Singer-Krüger et al., 2020), thus illustrating the higher efficiency of Alk-Ph labeling in yeast (Figures 3D and 3E). As a demonstration of the high spatial specificity of our dataset, we examined the coverage of TIM23 protein complex and OXPHOS protein complexes across the IMM (Bolender et al., 2008; Hartley et al., 2019; Kanehisa and Goto, 2000; Srivastava et al., 2018). As expected, only those subunits with matrix exposure can be detected in our dataset (Figure 3F; Table S6).

Recently, APEX2-mediated proximity-dependent biotinylation has been extended to profile the subcellular transcriptome (Fazal et al., 2019; Padrón et al., 2019; Zhou et al., 2019). Given its higher efficiency, we speculated that the Alk-Ph probe is also useful for labeling RNA in yeast. To evaluate the labeling efficiency toward yeast mitochondrial transcriptome, W303 cells expressing Su9-APEX2 were labeled with either Alk-Ph or BP at 2.5 mM final concentration. Following cell lysis and RNA extraction with TRIzol, the sample was digested with DNase I to remove residual DNA. For Alk-Ph-labeled samples, purified RNA was subsequently ligated with azide-$(PEG)_3$-biotin. Biotinylated RNA was enriched with streptavidin-coated beads, reverse-transcribed into cDNA, and quantitated by real-time PCR (Figure 4A).

We chose three mitochondrial mRNA (*MT-COX1*, *MT-ATP9*, *MT-ATP6*) and a mitochondrial rRNA (*MT-21S rRNA*) as our positive markers, and two abundant cytosolic mRNA, *ACT1* and *TDH3*, as negative markers. Real-time-PCR analysis revealed 2.2- to 4.3-fold enrichment of the four positive markers in Alk-Ph-labeled samples, relative to the negative marker, *ACT1*, whereas another negative marker *TDH3* was not significantly enriched (1.06 ± 0.43) (Figure 4B). Consistent with the low efficiency of BP in yeast, no substantial enrichment of positive RNA markers was observed in samples labeled with BP (Figure 4B). We further demonstrated that RNA enrichment depended on APEX2-mediated labeling, as negative control samples omitting APEX2 (cells expressing Su9-GFP), H_2O_2, or the probe, yielded minimum enrichment of mitochondrial genes (Figure S4). To the best of our knowledge, this is the first demonstration of proximity-dependent transcriptomic profiling in yeast.

DISCUSSION

To summarize, we have screened a panel of alkyne-modified aromatic APEX2 substrates for improved labeling efficiency in live yeast cells. Among these, Alk-Ph emerged as the most efficient probe, owing to a combination of high solubility, high permeability through the yeast cell wall, and a suitable redox potential for APEX2-mediated probe oxidation and protein labeling. In theory, electron-rich aromatic substrates are more readily oxidized by APEX2 into free radicals than electron-deficient substrates. Yet, the reactivity of the resulting free radical is negatively correlated with the electron density of the probe. These two competing factors suggest that a suitable range of redox potential may exist for the most efficient APEX2 probes. Notably, our observation that the simplest form of Alk-Ph yielded the highest labeling efficiency in yeast is consistent with previous reports that BP is the most efficient probe for APEX-mediated protein labeling in mammalian cells (Rhee et al., 2013; Zhou et al., 2019).

Our strategy avoids the harsh treatment with zymolase (Hwang and Espenshade, 2016) or freeze-thaw cycle (Singer-Krüger et al., 2020) to remove the yeast cell wall, which may introduce stress to cells and globally perturb the proteome. We applied this technique to investigate the sub-mitochondrial proteome, and our combined quantitative proteomic experiments identified 165 yeast mitochondrial matrix proteins with exceptional specificity (94%). Our protein-centric dataset contains eight proteins without prior mitochondrial annotations (Table S1), including two heat-shock proteins (HSP82 and HSP12) and four RNA-binding proteins (NPL3, GIS2, TIF3, PAB1). Among these, five proteins (PAB1, REG1, TIF3, STM1, HSP82) are close to the cutoff limit (Figure S2K) and are thus likely false positives. The remaining three proteins (NPL3, HSP12, GIS2) are not predicted to contain mitochondrial targeting sequences, as analyzed by MitoFates (Fukasawa et al., 2015), which warrants future investigations. We further extended Alk-Ph labeling to map the subcellular transcriptome in yeast. Our data demonstrate that APEX2-mediated Alk-Ph labeling is a generally applicable approach to profile the subcellular proteome and transcriptome in yeast, which could open up new avenues to study microorganisms with APEX2-mediated proximity labeling.

SIGNIFICANCE

This work offers an APEX2-based methodology that permits the proximity-dependent protein and RNA labeling in yeast. Through probe synthesis and activity screening, a clickable APEX2 substrate alkyne-phenol (Alk-Ph) is identified that exhibits enhanced labeling efficiency in intact yeast cells. Alk-Ph enables proteomic profiling in the mitochondrial matrix of intact yeast cells with exceptionally high specificity (94%), and offers higher coverage than the traditional APEX2 substrate biotin-phenol (BP). Alk-Ph also facilitates the identification of APEX-labeling sites, allowing the unambiguous assignment of membrane topology of mitochondrial proteins. This strategy has thus extended APEX2 applications to microorganisms.

SUPPORTING CITATIONS

The following references appear in the Supplemental Information: Rakestraw and Wittrup, 2006; Yofe et al., 2016.

STAR★METHODS

Detailed methods are provided in the online version of this paper and include the following:

- KEY RESOURCES TABLE
- RESOURCE AVAILABILITY
  - Lead Contact
  - Materials Availability
  - Data and Code Availability
- EXPERIMENTAL MODEL AND SUBJECT DETAILS
  - Yeast Strains, Media, Plasmids, and Strains Constructions
- METHOD DETAILS
  - Probe Synthesis
  - Yeast Transformation
  - Imaging of APEX2 Expression in Yeast Cells
  - Streptavidin Blot and In-Gel Fluorescence Characterization of APEX2 Labeling
  - Sample Preparation for Protein-Level Analysis
  - Sample Preparation for Site-Level Analysis
  - LC-MS/MS Analysis
  - Yeast RNA Labeling, Enrichment and Quantitation
- QUANTIFICATION AND STATISTICAL ANALYSIS
  - Protein Identification and Quantification
  - ROC Analysis to Determine the H/L Ratio Cut-Off

SUPPLEMENTAL INFORMATION

Supplemental Information can be found online at https://doi.org/10.1016/j.chembiol.2020.05.006.

ACKNOWLEDGMENTS

We thank Prof. Alice Ting (Stanford University) for providing pCTCON2 vector and for helpful discussions. This work was supported by the Ministry of Science and Technology, China (2017YFA0503600, 2018YFA0507600), the National Natural Science Foundation of China (91753131, 21673009, and 21727806), Natural Science Foundation of Beijing Municipality (5182011), the Interdisciplinary Medicine Seed Fund of Peking University (BMU2017MC006), State Key Laboratory of Proteomics (SKLP-K201804), and Li Ge-Zhao Ning Life Science Junior Research Fellowship. P.Z. was sponsored by the National Thousand Young Talents Award. We thank Profs. Tao Liu (Peking University), Ping Wei (Peking University), and Dr. Ping Xu (Beijing Proteome Research Center) for sharing yeast strains W303 and MHY500.

AUTHOR CONTRIBUTIONS

P.Z. and J.Y. conceived the project. P.Z. supervised APEX labeling and protein-centric proteomic experiments. J.Y. supervised peptide-centric proteomic experiments. Y.L., C.T., and Y.Z. performed all experiments. Y.L. synthesized the probes. Y.L., K.L., J.Y., and P.Z. analyzed the proteomic data. Y.L., Y.Z., and P.Z. analyzed RNA labeling data. Y.L., Y.Z., J.Y., and P.Z. wrote the paper with input from all authors.

DECLARATION OF INTERESTS

The authors declare no competing interests.

Received: January 9, 2019
Revised: March 24, 2019
Accepted: May 8, 2020
Published: May 28, 2020

REFERENCES

Beck, M., Topf, M., Frazier, Z., Tjong, H., Xu, M., Zhang, S., and Alber, F. (2011). Exploring the spatial and temporal organization of a cell's proteome. J. Struct. Biol. *173*, 483–496.

Bendayan, M. (2001). Worth its weight in gold. Science *291*, 1363–1365.

Bolender, N., Sickmann, A., Wagner, R., Meisinger, C., and Pfanner, N. (2008). Multiple pathways for sorting mitochondrial precursor proteins. EMBO Rep. *9*, 42–49.

Branon, T.C., Bosch, J.A., Sanchez, A.D., Udeshi, N.D., Svinkina, T., Carr, S.A., Feldman, J.L., Perrimon, N., and Ting, A.Y. (2018). Efficient proximity labeling in living cells and organisms with TurboID. Nat. Biotechnol. *36*, 880–887.

Chi, H., Liu, C., Yang, H., Zeng, W.F., Wu, L., Zhou, W.J., Wang, R.M., Niu, X.N., Ding, Y.H., Zhang, Y., et al. (2018). Comprehensive identification of peptides in tandem mass spectra using an efficient open search engine. Nat. Biotechnol. *36*, 1059–1061.

Choi-Rhee, E., Schulman, H., and Cronan, J.E. (2004). Promiscuous protein biotinylation by *Escherichia coli* biotin protein ligase. Protein Sci. *13*, 3043–3050.

Dennis, G., Sherman, B.T., Hosack, D.A., Yang, J., Gao, W., Lane, H.C., and Lempicki, R.A. (2003). DAVID: database for annotation, visualization, and integrated discovery. Genome Biol. *4*, R60.

Duina, A.A., Miller, M.E., and Keeney, J.B. (2014). Budding yeast for budding geneticists: a primer on the *Saccharomyces cerevisiae* model system. Genetics *197*, 33–48.

Fawcett, T. (2006). An introduction to ROC analysis. Pattern Recognit. Lett. *27*, 861–874.

Fazal, F.M., Han, S., Parker, K.R., Kaewsapsak, P., Xu, J., Boettiger, A.N., Chang, H.Y., and Ting, A.Y. (2019). Atlas of subcellular RNA localization revealed by APEX-seq. Cell *178*, 1–18.

Fu, L., Liu, K., Ferreira, R.B., Carroll, K.S., and Yang, J. (2019). Proteome-wide analysis of cysteine S-sulfenylation using a benzothiazine-based probe. Curr. Protoc. Protein Sci. *95*, e76.

Fukasawa, Y., Tsuji, J., Fu, S.-C., Tomii, K., Horton, P., and Imai, K. (2015). MitoFates: improved prediction of mitochondrial targeting sequences and their cleavage sites. Mol. Cell. Proteomics *14*, 1113.

Hartley, A.M., Lukoyanova, N., Zhang, Y., Cabrera-Orefice, A., Arnold, S., Meunier, B., Pinotsis, N., and Maréchal, A. (2019). Structure of yeast cytochrome c oxidase in a supercomplex with cytochrome bc1. Nat. Struct. Mol. Biol. *26*, 78–83.

Hsu, J.-L., Huang, S.-Y., Chow, N.-H., and Chen, S.-H. (2003). Stable-isotope dimethyl labeling for quantitative proteomics. Anal Chem. *75*, 6843–6852.

Hung, V., Zou, P., Rhee, H.-W., Udeshi, N.D., Cracan, V., Svinkina, T., Carr, S.A., Mootha, V.K., and Ting, A.Y. (2014). Proteomic mapping of the human mitochondrial intermembrane space in live cells via ratiometric APEX tagging. Mol. Cell *55*, 332–341.

Hung, V., Udeshi, N.D., Lam, S.S., Loh, K.H., Cox, K.J., Pedram, K., Carr, S.A., and Ting, A.Y. (2016). Spatially resolved proteomic mapping in living cells with the engineered peroxidase APEX2. Nat. Protoc. *11*, 456–475.

Hung, V., Lam, S.S., Udeshi, N.D., Svinkina, T., Guzman, G., Mootha, V.K., Carr, S.A., and Ting, A.Y. (2017). Proteomic mapping of cytosol-facing outer mitochondrial and ER membranes in living human cells by proximity biotinylation. Elife *6*, e24463.

Hwang, J., and Espenshade, P.J. (2016). Proximity-dependent biotin labelling in yeast using the engineered ascorbate peroxidase APEX2. Biochem. J. *473*, 2463–2469.

Kalderon, D., Roberts, B.L., Richardson, W.D., and Smith, A.E. (1984). A short amino acid sequence able to specify nuclear location. Cell *39*, 499–509.

Kanehisa, M., and Goto, S. (2000). KEGG: Kyoto Encyclopedia of Genes and Genomes. Nucleic Acids Res. *28*, 27–30.

Kim, D.I., and Roux, K.J. (2016). Filling the void: proximity-based labeling of proteins in living cells. Trends Cell Biol. *26*, 804–817.

Kim, H.-Y.H., Tallman, K.A., Liebler, D.C., and Porter, N.A. (2009). An azido-biotin reagent for use in the isolation of protein adducts of lipid-derived electrophiles by streptavidin catch and photorelease. Mol. Cell. Proteomics *8*, 2080–2089.

Lam, S.S., Martell, J.D., Kamer, K.J., Deerinck, T.J., Ellisman, M.H., Mootha, V.K., and Ting, A.Y. (2015). Directed evolution of APEX2 for electron microscopy and proximity labeling. Nat. Methods *12*, 51–54.

Lee, S.-Y., Kang, M.-G., Shin, S., Kwak, C., Kwon, T., Seo, J.K., Kim, J.-S., and Rhee, H.-W. (2017). Architecture mapping of the inner mitochondrial membrane proteome by chemical tools in live cells. J. Am. Chem. Soc. *139*, 3651–3662.

Liu, C., Song, C.Q., Yuan, Z.F., Fu, Y., Chi, H., Wang, L.H., Fan, S.B., Zhang, K., Zeng, W.F., He, S.M., et al. (2014). pQuant improves quantitation by keeping out interfering signals and evaluating the accuracy of calculated ratios. Anal. Chem. *86*, 5286–5294.

Markmiller, S., Soltanieh, S., Server, K.L., Mak, R., Jin, W., Fang, M.Y., Luo, E.-C., Krach, F., Yang, D., Sen, A., et al. (2018). Context-dependent and disease-specific diversity in protein interactions within stress granules. Cell *172*, 590–604.

Mayer, G., and Bendayan, M. (1997). Biotinyl-tyramide: a novel approach for electron microscopic immunocytochemistry. J. Histochem. Cytochem. *45*, 1449–1454.

Mortensen, A., and Skibsted, L.H. (1997). Importance of carotenoid structure in radical-scavenging reactions. J. Agric. Food Chem. *45*, 2970–2977.

Padrón, A., Iwasaki, S., and Ingolia, N.T. (2019). Proximity RNA labeling by APEX-seq reveals the organization of translation initiation complexes and repressive RNA granules. Mol. Cell *75*, 875–887.

Paek, J., Kalocsay, M., Staus, D.P., Wingler, L., Pascolutti, R., Paulo, J.A., Gygi, S.P., and Kruse, A.C. (2017). Multidimensional tracking of GPCR signaling via peroxidase-catalyzed proximity labeling. Cell *169*, 338–349.

Pan, Y. (2011). Mitochondria, reactive oxygen species, and chronological aging: a message from yeast. Exp. Gerontol. *46*, 847–852.

Rakestraw, A., and Wittrup, K.D. (2006). Contrasting secretory processing of simultaneously expressed heterologous proteins in *Saccharomyces cerevisiae*. Biotechnol. Bioeng. *93*, 896–905.

Rhee, H.-W., Zou, P., Udeshi, N.D., Martell, J.D., Mootha, V.K., Carr, S.A., and Ting, A.Y. (2013). Proteomic mapping of mitochondria in living cells via spatially restricted enzymatic tagging. Science *339*, 1328–1331.

Santin, Y.G., Doan, T., Lebrun, R., Espinosa, L., Journet, L., and Cascales, E. (2018). In vivo TssA proximity labelling during type VI secretion biogenesis reveals TagA as a protein that stops and holds the sheath. Nat. Microbiol. *3*, 1304–1313.

Singer-Krüger, B., Fröhlich, T., Franz-Wachtel, M., Nalpas, N., Macek, B., and Jansen, R.-P. (2020). APEX2-mediated proximity labeling resolves protein networks in *Saccharomyces cerevisiae* cells. FEBS J. *287*, 325–344.

Srivastava, A.P., Luo, M., Zhou, W., Symersky, J., Bai, D., Chambers, M.G., Faraldo-Gómez, J.D., Liao, M., and Mueller, D.M. (2018). High-resolution cryo-EM analysis of the yeast ATP synthase in a lipid membrane. Science *360*, eaas9699.

The UniProt, C. (2014). UniProt: a hub for protein information. Nucleic Acids Res. *43*, D204–D212.

Udeshi, N.D., Pedram, K., Svinkina, T., Fereshetian, S., Myers, S.A., Aygun, O., Krug, K., Clauser, K., Ryan, D., Ast, T., et al. (2017). Antibodies to biotin enable large-scale detection of biotinylation sites on proteins. Nat. Methods *14*, 1167–1170.

Vögtle, F.N., Burkhart, J.M., Gonczarowska-Jorge, H., Kücükköse, C., Taskin, A.A., Kopczynski, D., Ahrends, R., Mossmann, D., Sickmann, A., Zahedi, R.P., et al. (2017). Landscape of submitochondrial protein distribution. Nat. Commun. *8*, 290.

Westermann, B., and Neupert, W. (2000). Mitochondria-targeted green fluorescent proteins: convenient tools for the study of organelle biogenesis in *Saccharomyces cerevisiae*. Yeast *16*, 1421–1427.

Williamson, D.H., and Fennell, D.J. (1979). Visualization of yeast mitochondrial DNA with the fluorescent stain "DAPI". Methods Enzymol. *56*, 728–733.

Wilson, W.A., Boyer, M.P., Davis, K.D., Burke, M., and Roach, P.J. (2010). The subcellular localization of yeast glycogen synthase is dependent upon glycogen content. Can. J. Microbiol. *56*, 408–420.

Yang, J., Gupta, V., Tallman, K.A., Porter, N.A., Carroll, K.S., and Liebler, D.C. (2015). Global, in situ, site-specific analysis of protein S-sulfenylation. Nat. Protoc. *10*, 1022–1037.

Yofe, I., Weill, U., Meurer, M., Chuartzman, S., Zalckvar, E., Goldman, O., Ben-Dor, S., Schütze, C., Wiedemann, N., Knop, M., et al. (2016). One library to make them all: streamlining the creation of yeast libraries via a SWAp-Tag strategy. Nat. Methods *13*, 371–378.

Zhou, Y., Wang, G., Wang, P., Li, Z., Yue, T., Wang, J., and Zou, P. (2019). Expanding APEX2 substrates for proximity-dependent labeling of nucleic acids and proteins in living cells. Angew. Chem. Int. Ed. *58*, 11763–11767.

Please cite this article in press as: Li et al., A Clickable APEX Probe for Proximity-Dependent Proteomic Profiling in Yeast, Cell Chemical Biology (2020), https://doi.org/10.1016/j.chembiol.2020.05.006

CellPress

STAR★METHODS

KEY RESOURCES TABLE

REAGENT or RESOURCE	SOURCE	IDENTIFIER
Antibodies		
Streptavidin HRP	Pierce	Cat# 21124
Flag-Tag Monoclonal Antibody (2C5)	Biodragon	Cat# B1001
Anti: GFP antibody	Abcam	Cat# Ab290; RRID: AB_303395
HRP-Goat Anti-Mouse IgG (H+L)	Ruiying	Cat# RS0001
HRP-Goat Anti-Rabbit IgG (H+L)	Ruiying	Cat# RS0002
Chemicals, Peptides, and Recombinant Proteins		
Phanta® Max Super-Fidelity DNA Polymerase	Vazyme	Cat# P505-d2
Gibson Assembly Master Mix	NEB	Cat# E2611S
2×Pfu MasterMix (Dye)	Cwbio	Cat# CW0686A
D-(+)-Glucose	Sigma	Cat# G6152-500G
Yeast Nitrogen Base without Amino Acids	BD	Cat# 291940
Yeast Synthetic Drop-out Medium Supplements without uracil, leucine, and tryptophan	Sigma	Cat# Y1876
D-(+)-Galactose	Amresco	Cat# 0637
Peptone	Amresco	Cat# J636
Yeast Extract	OXOID	Cat# LP0021
4-Pentynoic acid	Ark	Cat# AK-32594
N-Hydroxysuccinimide	J&K	Cat# 117997
1-(3-dimethylaminopropyl)-3-ethylcarbodiimide hydrochloride	J&K	Cat# 211112
Tyramine	J&K	Cat# 953409
Triethylamine	J&K	Cat# 432915
2-(4-Aminophenyl) ethylamine	J&K	Cat# 311466
3-Hydroxybenzoic acid	J&K	Cat# 163105
2-Propynylamine	TCI	Cat# P0911
4-Hydroxybenzoic acid	J&K	Cat# 506842
1-Hydroxybenzotriazole	J&K	Cat# 191943
5-hydroxynicotinic acid	J&K	Cat# 258273
DAPI	Thermo Fisher	Cat# D1306
Hoechst 33342	Bioworld	Cat# BD5013
Tetramethylrhodamine methyl ester	AAT Bioquest	Cat# 22221
Sodium ascorbate	Aladdin	Cat# S105024
6-Hydroxy-2,5,7,8-tetramethylchroman-2-carboxylic acid (Trolox)	Sigma	Cat# 238813
Protease Inhibitor Cocktail (100×)	Cwbio	Cat# CW2200S
Glass beads	Sigma	Cat# G8772
Biotin-$(PEG)_3$-Azide	Click Chemistry Tools	Cat# AZ104
Cy5 Azide	Click Chemistry Tools	Cat# AZ118
BTTAA	Click Chemistry Tools	Cat# 1236
THPTA	Click Chemistry Tools	Cat# 1010
Copper sulfate pentahydrate	Aladdin	Cat# C112401
Pierece Streptavidin Agarose	Pierece	Cat# 20349
Trpysin	Promega	Cat# V5111
Dithiothreitol	Sigma	Cat# D9163

(*Continued on next page*)

Please cite this article in press as: Li et al., A Clickable APEX Probe for Proximity-Dependent Proteomic Profiling in Yeast, Cell Chemical Biology (2020), https://doi.org/10.1016/j.chembiol.2020.05.006

Continued

REAGENT or RESOURCE	SOURCE	IDENTIFIER
Iodoacetamide	Sigma	Cat# I6125
Triethylammonium bicarbonate buffer	Sigma	Cat# T7408
Formaldehyde solution	Sigma	Cat# 252549
Formaldehyde solution ^{13}C, d_2	Sigma	Cat# 596388
Formic acid	Aladdin	Cat# F112032
HLB extraction cartridges	Waters	Cat# 186000383
Streptavidin Sepharose high performance	GE	Cat# 17-5113-01
Phosphate-Buffered Saline (10X) pH 7.4, RNase-free	Invitrogen	Cat# AM9624
BeyoPure™ Ultrapure Water (DNase/RNase-Free, Sterile)	BeyoPure	Cat# ST876
TRIzol™ Reagent	Life Technologies	Cat# 15596018
DNase I (RNase-free)	NEB	Cat# M0303
Dynabeads® MyOne™ Streptavidin C1	Invitrogen	Cat# 65002
UltraPure™ 1 M Tris-HCl Buffer, pH 7.5	Invitrogen	Cat# 15567-027
NaCl (5 M), RNase-free	Invitrogen	Cat# AM9759
EDTA (0.5 M), pH 8.0, RNase-free	Invitrogen	Cat# AM9260G
TWEEN® 20	Sigma	Cat# P1379
Sodium hydroxide solution	Sigma	Cat# S2770-100ML
Bovine serum albumin, fraction V, heat shock isolation	Sangon Biotech	Cat# A500023-0100
Yeast tRNA	Invitrogen	Cat# 15401-011
Urea	Sigma	Cat# U5378
SDS, 10% Solution, RNase-free	Invitrogen	Cat# AM9822
Formamide	Sigma	Cat# F9037
D-Biotin	Invitrogen	Cat# B20656
PowerUp™ SYBR™ Green Master Mix	Applied Biosystems	Cat# A25778
Probe **1**	This paper	N/A
Probe **2**	This paper	N/A
Probe **3**	This paper	N/A
Probe **4**	This paper	N/A
Probe **5**	This paper	N/A
Probe **6**	Laboratory of Prof. Chu Wang	N/A
Probe **7**	Laboratory of Prof. Chu Wang	N/A
Probe **8**	Laboratory of Prof. Chu Wang	N/A
Critical Commercial Assays		
DNA extraction kit	TIANGEN	Cat# DP118-02
Frozen-EZ Yeast Transformation II Kit™	zymo research	Cat# T2001
BCA Protein Assay Kit	Pierece	Cat# 23227
RNA Clean & Concentrator-100 Kit	Zymo	Cat# R1019
ProtoScript® II First Strand cDNA Synthesis Kit	NEB	Cat# E6560
Experimental Models: Organisms/Strains		
S. cerevisiae: Strain W303 (*MATa*)	Laboratory of Prof. Tao Liu and Ping Wei	N/A
S. cerevisiae: Strain MHY500 (*MATa*)	Laboratory of Prof. Ping Xu	N/A
Oligonucleotides		
Primer for pCTCON2-Su9-APEX2-eGFP fwd: CCCCGGATCGAATTCCCTACTTCA rev: CTTGTACAGCTCGTCCATGCCG	This paper	N/A
Primer for pCTCON2-Su9-eGFP fwd: CCCCGGATCGAATTCCCTACTTCA rev: CTTGTACAGCTCGTCCATGCCG	This paper	N/A

(*Continued on next page*)

Please cite this article in press as: Li et al., A Clickable APEX Probe for Proximity-Dependent Proteomic Profiling in Yeast, Cell Chemical Biology (2020), https://doi.org/10.1016/j.chembiol.2020.05.006

Continued

REAGENT or RESOURCE	SOURCE	IDENTIFIER
Primer for pCTCON2-NLS-APEX2-eGFP fwd: ATGCCACCAAAAAAAAAAAGAAAAGTTAAGG ACAATAGCTCGACGATTG rev: GATCCGCTAGCACCAGAGCCTC	This paper	N/A
Primer for pCTCON2-Aga2p-APEX2 fwd: AATATACCTCTATACTTTAACGTC rev: TGTAAAACGACGGCCAGT	This paper	N/A
RT-PCR primer for *ACT1* gene fwd: GAAATGCAAACCGCTGCTCA rev: TACCGGCAGATTCCAAACCC	This paper	N/A
RT-PCR primer for *TDH3* gene fwd: TCACGGTAGATACGCTGGTG rev: CCAGCGTCAATGTGCTTTTG	This paper	N/A
RT-PCR primer for *MT-COX1* gene fwd: GTGGTTTAACTGGTGTTGCCT rev: GTGAAAATGTCCCACCACGTA	This paper	N/A
RT-PCR primer for *MT-ATP6* gene fwd: TGCTTAAAGGACAAATTGGAGGTAA rev: CCAGCAGGTACGAATAATGAGA	This paper	N/A
RT-PCR primer for *MT-ATP9* gene fwd: TTGCTATCGTATTCGCAGCTTT rev: AGCTTCTGATAAGGCGAAACC	This paper	N/A
RT-PCR primer for *MT-21S rRNA* gene fwd: AGCGAAATTCCTTGGCCTATAA rev: CCGTCTTGCTGAAGGTACATAG	This paper	N/A
Recombinant DNA		
pCTCON2	Laboratory of Prof. Alice Ting	N/A
Software and Algorithms		
pFind studio (Version 3.0.11)	Chi et al., 2018	http://pfind.ict.ac.cn/software/pFind3/index.html
pQuant	Liu et al., 2014	http://pfind.ict.ac.cn/software/pFind3/index.html

RESOURCE AVAILABILITY

Lead Contact

Further information and requests for resources and reagents should be directed to and will be fulfilled by the Lead Contact, Peng Zou (zoupeng@pku.edu.cn).

Materials Availability

All unique/stable reagents generated in this study are available from the Lead Contact with a completed Materials Transfer Agreement.

Data and Code Availability

All data presented are available in the main text and Supplemental Information.

EXPERIMENTAL MODEL AND SUBJECT DETAILS

Yeast Strains, Media, Plasmids, and Strains Constructions

S. cerevisiae W303 strain (*MATa leu2-3, 112 trp1-1 can1-100 ura3-1 ade2-1 his3-11, 15*)[*phi*$^{+}$] was a gift from Profs. Tao Liu and Ping Wei (Peking University). *S. cerevisiae* MHY500 strain (*MATa his3 200 leu2-3,112 ura3-52 lys2-801 trp1-1*) was a gift from Dr. Ping Xu (Phoenix Center in Beijing). Yeast cells were grown in the synthetic drop-out medium without tryptophan (SD media, containing 20 g/L glucose, 6.7 g/L yeast nitrogen base and 1.92 g/L yeast synthetic drop-out medium supplements without tryptophan) to mid-log phase at 30°C on a rotary shaker. W303 and MHY500 cells were transformed with plasmids using the EZ frozen transformation kit (Zymo Research) following manufacturer's instructions. Protein expression was induced by yeast extract peptone galactose media (YPG media, containing 20 g/L galactose, 20 g/L peptone and 10 g/L yeast extract) or synthetic galactose minimal medium

Please cite this article in press as: Li et al., A Clickable APEX Probe for Proximity-Dependent Proteomic Profiling in Yeast, Cell Chemical Biology (2020), https://doi.org/10.1016/j.chembiol.2020.05.006

without tryptophan (SG media, containing 20 g/L galactose, 6.7 g/L yeast nitrogen base and 1.92 g/L yeast synthetic drop-out medium supplements without tryptophan).

METHOD DETAILS

Probe Synthesis

Synthesis of Probe 1

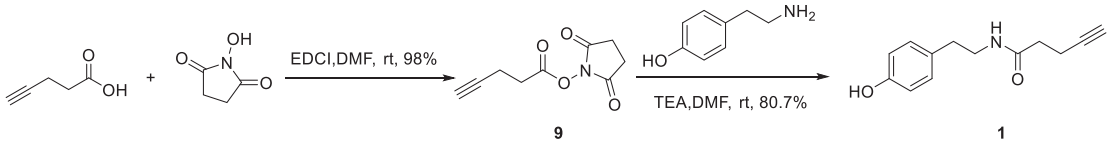

Compound **9** was prepared by adding 4-pentynoic acid (0.245 g, 2.5 mmol, Ark), N-hydroxysuccinimide (0.288 g, 2.5 mmol) and 1-(3-dimethylaminopropyl)-3-ethylcarbodiimide hydrochloride1-(3-dimethylaminopropyl)-3-ethylcarbodiimide hydrochloride (0.613 g, 3.2 mmol) to 20 mL anhydrous DMF. The reaction mixture was stirred overnight at room temperature. After the solvent was removed under vacuum, yellow residue was diluted with 15 mL ethyl acetate and 5 mL water. The combined organic layer was washed with 5 mL dilute hydrochloric acid solution (pH ~ 4), water and brine successively, dried over sodium sulfate and concentrated. The crude mixture was purified by silica gel chromatography (1% methanol in DCM) to obtain a white solid. The yield was 98%. ^{1}H NMR (400 MHz, d_6-DMSO): 2.90 (m, 4H), 2.81(s, 4H), 2.50 (d, 2H).

Probe **1** was prepared by mixing compound **9** (0.24 g, 1,23 mmol), tyramine (0.342 g, 2.5 mmol) and triethylamine (860 μL, 6.2 mmol) in 15 mL DMF. The reaction mixture was stirred overnight at room temperature. After the solvent was removed under vacuum, product was extracted by 3x10 mL ethyl acetate. The combined organic layer was washed with 5 mL dilute hydrochloric acid solution (pH ~ 4), water and brine successively, dried over sodium sulfate and concentrated. The crude mixture was purified by silica gel chromatography (2% methanol in DCM) to obtain a white solid. The yield was 81%. ^{1}H NMR (400 MHz, d_6-DMSO): 9.16 (s, 1H), 7.93 (t, J = 5.7 Hz, 1H), 7.04 – 6.95 (m, 2H), 6.71 – 6.62 (m, 2H), 3.24 – 3.14 (m, 2H), 2.81 – 2.71 (m, 1H), 2.57 (t, J = 7.5 Hz, 2H), 2.33 (td, J = 6.8, 2.4 Hz, 2H), 2.24 (dd, J = 7.7, 6.1 Hz, 2H). Calculated m/z for $C_{13}H_{15}NO_2$: $[M+H]^+$, 218.27; found 218.51.

Synthesis of Probe 2

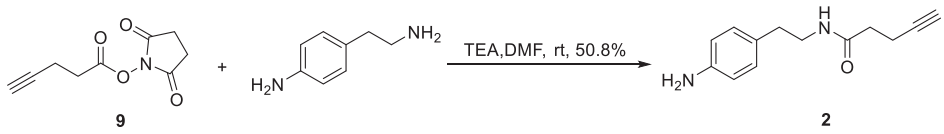

Probe **2** was prepared by mixing compound **9** (0.244 g, 1.23 mmol), 2-(4-aminophenyl) ethylamine (0.340 g, 2.5 mmol) and triethylamine (860 μL, 6.2 mmol) in 15 mL DMF. The reaction mixture was stirred overnight at room temperature. After the solvent was removed under vacuum, product was extracted by 3x10 mL ethyl acetate. The combined organic layer was washed with 5 mL dilute hydrochloric acid solution (pH ~ 4), water and brine successively, dried over sodium sulfate and concentrated. The crude mixture was purified by silica gel chromatography (2.5% methanol in DCM) to obtain a light yellow solid. The yield was 51%. ^{1}H NMR (400 MHz, d_6-DMSO): 9.71(t, 1H, J = 5.7Hz), 6.87 – 6.80 (m, 2H), 6.51 – 6.44 (m, 2H), 4.85 (s, 2H), 3.15 (dt, J = 8.2, 6.1 Hz, 2H), 2.76 (t, J = 2.6 Hz, 1H), 2.50 (t, J = 4.8Hz, 2H, d), 2.34 (td, J = 7.5, 6.5, 2.0 Hz, 2H), 2.24 (dd, J = 7.8, 6.1 Hz, 2H). Calculated m/z for $C_{13}H_{16}N_2O$: $[M+H]^+$, 217.28; found, 217.10.

Synthesis of Probe 3

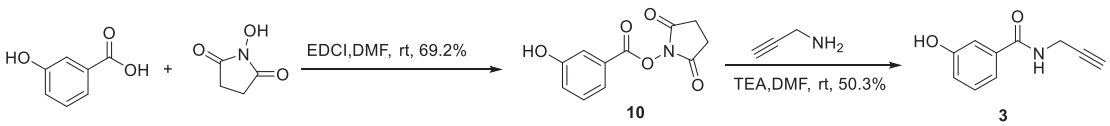

Compound **10** was prepared by adding 3-hydroxybenzoic acid (0.500 g, 3.62 mmol), N-hydroxysuccinimide (0.417 g, 3.62 mmol) and 1-(3-dimethylaminopropyl)-3-ethyl-carbodiimide hydrochloride (0.785 g, 4.71 mmol) to 30 mL anhydrous DMF. The reaction mixture was stirred overnight at room temperature. After the solvent was removed under vacuum, product was extracted by 3x10 mL DCM. The combined organic layer was washed with 5 mL water for three times, dried over sodium sulfate and concentrated. The crude mixture was purified by silica gel chromatography (1:1 PE/EA) to obtain a white solid. The yield was 69%.

Please cite this article in press as: Li et al., A Clickable APEX Probe for Proximity-Dependent Proteomic Profiling in Yeast, Cell Chemical Biology (2020), https://doi.org/10.1016/j.chembiol.2020.05.006

Probe **3** was prepared by dissolving compound **10** (0.300 g, 1,28 mmol) in 15 mL DMF, adding 2-propynylamine (820 μL, 12.8 mmol) and triethylamine (530 μL, 3.83mmol). The reaction mixture was stirred overnight at room temperature. After the solvent was removed under vacuum, product was extracted by 3x10 mL ethyl acetate. The combined organic layer was washed with 5 mL dilute hydrochloric acid solution (pH ~ 4), water and brine successively, dried over sodium sulfate and concentrated. The crude mixture was purified by silica gel chromatography (1:1 PE/EA) to obtain white solid. The yield was 50.3%. ^{1}H NMR (400 MHz, d_6-DMSO): 9.66 (s, 1H), 8.81 (t, J = 5.6 Hz, 1H), 7.31 – 7.16 (m, 3H), 6.91 (dt, J = 6.3, 2.7 Hz, 1H), 4.01 (dd, J = 5.6, 2.6 Hz, 2H), 3.10 (t, J = 2.5 Hz, 1H). Calculated m/z for $C_{10}H_9NO_2$: $[M+H]^+$, 176.19; found, 175.98.

Synthesis of Probe 4

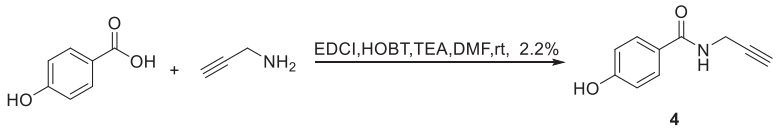

4

Probe **4** was prepared by mixing 4-hydroxybenzoic acid (0.300 g, 2.17 mmol), 2-propynyl-amine (120 μL, 2.17 mmol), 1-(3-dimethylaminopropyl)-3-ethylcarbodiimide hydrochloride (0.500 g, 2.60 mmol), 1-hydroxybenzotriazole (0.353 g, 2.60 mmol) and triethylamine (750 μL, 5.42 mmol) to 20 mL anhydrous DMF. The reaction mixture was stirred overnight at room temperature. After the solvent was removed under vacuum, product was extracted by 3x10 mL ethyl acetate. The combined organic layer was washed with 5 mL water for three times, dried over sodium sulfate and concentrated. The crude mixture was purified by C18 reverse column chromatography (20% methanol in water) to obtain white solid. The yield was 2.2%. ^{1}H NMR (400 MHz, d_6-DMSO): 8.64 (s, 1H), 7.72 (d, J = 8.6 Hz, 2H), 6.79 (d, J = 8.6 Hz, 2H), 4.01 (dd, J = 5.8, 2.5 Hz, 2H), 3.08 (m,1H).

Synthesis of Probe 5

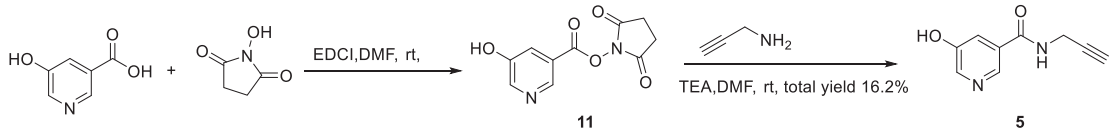

11 5

Compound **11** was prepared by adding 5-hydroxynicotinic acid (0.250 g, 1.81 mmol), N-hydroxysuccinimide (0.212 g, 1.81 mmol) and 1-(3-dimethylaminopropyl)-3-ethylcarbodi-imide hydrochloride (0.446 g, 2.35 mmol) to 20 mL anhydrous DMF. The reaction mixture was stirred overnight at room temperature. After the solvent was removed under vacuum, product was extracted by 3x10 mL DCM. The combined organic layer was washed with 5 mL water for three times, dried over sodium sulfate and concentrated. The crude mixture was purified by silica gel chromatography (1:1 PE/EA) to obtain oily liquid.

Probe **3** was prepared by dissolving preceding compound 11 in 15 mL DMF, adding 2-propynylamine (1 mL, 15.6 mmol) and triethylamine (600 μL, 4.34 mmol). The reaction mixture was stirred overnight at room temperature. After the solvent was removed under vacuum, product was extracted by 3x10 mL ethyl acetate. The combined organic layer was washed with 5 mL dilute hydrochloric acid solution (pH ~ 4), water and brine successively, dried over sodium sulfate and concentrated. The crude mixture was purified by silica gel chromatography (1:1 PE/EA) to obtain a white solid. The total yield was 16%. ^{1}H NMR (400 MHz, d_6-DMSO): 10.24 (s, 1H), 9.05 (t, J = 5.5 Hz, 1H), 8.47 (d, J = 1.8 Hz, 1H), 8.26 (d, J = 2.8 Hz, 1H), 7.53 (dd, J = 2.8, 1.9 Hz, 1H), 4.05 (dd, J = 5.5, 2.5 Hz, 2H), 3.15 (t, J = 2.5 Hz, 1H). Calculated m/z for $C_9H_8N_2O_2$: $[M+H]^+$,177.18; found 177.25.

Yeast Transformation

Wild type-W303 or MHY500 strain cells were grown at 30°C to mid-log phase in 10 mL yeast extract peptone dextrose medium (YPD medium, containing 20 g/L glucose, 20 g/L peptone and 10 g/L yeast extract). The cells were pelleted at 500 g for 4 min and the supernatant was discarded. 10 mL EZ 1 solution (from the EZ frozen transformation kit, Zymo Research) was added to wash the pellet. The supernatant was discarded again after centrifugation at 500 g for 4 min. The competent cells were obtained by resuspending the cell pellet in 1 mL EZ 2 solution (from the EZ frozen transformation kit, Zymo Research). 20 μL of competent cells were mixed with 0.1-0.5 μg plasmid DNA (in less than 2 μL volume) and 200 μL EZ 3 solution (from the EZ frozen transformation kit, Zymo Research). The mixture was vortexed thoroughly and incubated at 30°C for 1.5 h. The transformation solution was mixed vigorously for three times during the incubation. The above transformation mixture was spread on a synthetic drop-out medium plate without tryptophan (SD plate, containing 20 g/L glucose, 15 g/L agar, 6.7 g/L yeast nitrogen base and 1.92 g/L yeast synthetic drop-out medium supplements without tryptophan) and incubated at 30°C for two days.

Imaging of APEX2 Expression in Yeast Cells

All transformants were grown to mid-log phase in SD cell culture and subsequently were inoculated into SG cell culture. Cells were harvested at mid-log phase, washed with PBS buffer twice for confocal imaging. To stain yeast mitochondria, harvested cells were incubated with 5 mg/mL DAPI dye in PBS buffer for 30 min at 30°C (Williamson and Fennell, 1979) or 2 μM tetramethylrhodamine

Please cite this article in press as: Li et al., A Clickable APEX Probe for Proximity-Dependent Proteomic Profiling in Yeast, Cell Chemical Biology (2020), https://doi.org/10.1016/j.chembiol.2020.05.006

methyl ester (TMRM) dye in PBS buffer for 1 h. To stain the yeast nucleus, harvested cells were incubated with 5 mM Hoechst 33342 (Bioworld) in PBS buffer for 30 min at 30°C (Wilson et al., 2010). Stained cells were imaged on a ZEISS LSM 700 laser scanning confocal microscope.

Streptavidin Blot and In-Gel Fluorescence Characterization of APEX2 Labeling

All transformants were grown to mid-log phase in SD cell culture and subsequently were inoculated into SG cell culture or YPG culture. Cells were harvested at mid-log phase, washed with PBS buffer twice. Cell pellets were re-suspended at 2.5 mM Alk-Ph in PBS buffer (about 500 μL Alk-Ph solution for 5 OD_{600} yeast cells) and incubated for 30 min at room temperature. Then H_2O_2 (C_f 1 mM) was added for 1 min to trigger the generation of phenol radical and APEX2 labeling. An equal volume of quencher solution consisting 10 mM sodium azide, 10 mM sodium ascorbate and 5 mM trolox in PBS buffer was added to stop Alk-Ph labeling. After APEX2 labeling, cells were washed with PBS buffer twice and resuspended in PBS buffer with protease inhibitor cocktail (Cowin). Cells were then mixed with an equal volume glass beads (Sigma) and vibrated at 2000 rpm at 4°C for 1 min. Thereafter, cells were cooled on ice for 1 min. The "shake-cool" cycle was repeated for 10 times to lyse yeast cells. Excess small molecules were removed by protein precipitation in cold methanol at -80°C for 3 h.

The protein pellet was resuspended in 0.5% SDS in water, then clicked with azide-$(PEG)_3$-biotin reagent (C_f 100 μM) or azide-Cy5 (C_f 100 μM) in the presence of $CuSO_4$ (C_f 333 μM), BTTAA (C_f 666 μM) and sodium ascorbate (C_f 2.5 mM) for 1 h at room temperature. Labeled protein samples were separated on a 12% SDS-PAGE gel.

For in-gel fluorescence analysis, gels were rinsed with destaining solution (60% v/v water, 30% v/v methanol, 10% v/v acetic acid) and followed by imaging on Typhoon FLA 9500 imager. For blotting analysis, gels were transferred to nitrocellulose membrane (Bio-Rad) and blocked by 3% BSA in TBST buffer (TBS buffer with 0.1% Tween20) at 4°C overnight. The blots were immersed with 0.25 μg/ml streptavidin-HRP (Thermo Fisher Scientific) at room temperature for 1 h. For detecting the expression of Flag or GFP, the blots were probed with α-Flag monoclonal antibody (Biodragon) or rabbit α-GFP (Abcam) as primary antibodies, followed by HRP-conjugated goat α-mouse IgG or α-rabbit IgG as the secondary antibodies. Chemiluminescence imaging of the blots were performed on a Chemidoc imager (Bio-Rad).

Sample Preparation for Protein-Level Analysis

60 OD_{600} yeast cells expressing Su9-APEX2-Flag-eGFP or Su9-Flag-eGFP at mid-log phase were harvested, followed by APEX2 labeling, cell lysis and click chemistry (with Biotin-$(PEG)_3$-Azide) as previously described. About 1.5 mg proteins were quantified by BCA assay (Pierce, Thermo Fisher Scientific) for each control group (from 60 OD_{600} yeast). Excess small molecules were removed by protein precipitation in cold methanol at -80°C for 3 h. Protein pellet was resuspended in 100 μL 0.5% SDS in water, incubated with 200 uL streptavidin agarose beads (Thermo Fisher) at room temperature for 2 h with gently rotation, and then were washed extensively, twice with 1 mL 2% SDS in water, twice with 1 mL 8 M urea, and twice with 1 mL 2 M sodium chloride.

Prior to on-beads digestion, proteins on the beads were incubated with 0.3 M urea and 10 mM dithiothreitol at 60°C for 15 min and alkylated with 20 mM iodoacetamide in the dark at 35°C for 30 min. Beads were washed twice with triethylammonium bicarbonate buffer (Sigma) to remove excess small molecules and then treated with 4 μg sequencing-grade trypsin (Promega) for 16 h at 37°C to digest proteins into peptides. Thereafter, released peptides were collected from the supernatant following centrifugation at 15000 g for 10 min at 4°C, and the beads pellet was discarded.

For dimethylation, each peptide sample (200 μL) was mixed with 12 μL 4% (v/v) CH_2O (Sigma) or 12 μL 4% (v/v) CD_2O (Sigma), respectively, and 12 μL $NaBH_3CN$. The solution was incubated at room temperature for 1 h. After adding 48 μL 1% (v/v) ammonia solution (Aladdin) and 24 μL formic acid (Sigma), the light and heavy isotopically labeled samples were mixed and desalted with HLB extraction cartridges (Waters) as previously described (Fu et al., 2019; Yang et al., 2015).

Sample Preparation for Site-Level Analysis

60 OD_{600} yeast cells expressing Su9-APEX2-Flag-eGFP or Su9-Flag-eGFP at mid-log phase were harvested, followed by APEX2 labeling, cell lysis as previously described. The protein samples were further incubated with 8 mM dithiothreitol (DTT, Research Products International) at 25°C for 1 h and then alkylated with 32 mM iodoacetamide in the dark at 25°C for additional 30 min. Excess small molecules were removed by protein precipitation using methanol-chloroform system (aqueous phase/methanol/chloroform, 4:4:1 (v/v/v)) as previously described (Fu et al., 2019; Kim et al., 2009; Yang et al., 2015). The precipitated proteins were resuspended with 50 mM ammonium bicarbonate containing 0.2 M urea with sonication. Resuspended protein concentrations were determined with the BCA assay (Pierce, Thermo Fisher Scientific) and adjusted to a concentration of 1 mg/mL. Resuspended proteins were digested with sequencing-grade trypsin (Promega) at a 1:50 (enzyme/substrate) ratio overnight (~16 h) at 37°C.

The tryptic digests were desalted with HLB extraction cartridges (Waters) as previously described (Fu et al., 2019; Yang et al., 2015), dried by SpeedVac, and reconstituted in a solution containing 30% acetonitrile (ACN) at pH ~6. CuAAC reaction was performed by the addition of 1 mM either light or heavy Azido-UV-biotin, 10 mM sodium ascorbate, 1 mM TBTA, and 10 mM $CuSO_4$. After a 2 h incubation at 25°C with rotation and light protection, the light and heavy isotopic tagged samples were mixed equally. To remove the excess reactants, the peptide samples were cleaned by strong cation exchange (SCX) spin columns as previously described (Fu et al., 2019; Yang et al., 2015), and then allowed to interact with pre-washed streptavidin beads (GE). After a 2 h incubation at 25°C, the beads were washed with 50 mM NaAc (pH 4.5), 50 mM NaAc containing 2 M NaCl (pH 4.5), and water twice each to remove non-specific binding substances. Then, the beads were resuspended in 25 mM ammonium bicarbonate, transferred

Please cite this article in press as: Li et al., A Clickable APEX Probe for Proximity-Dependent Proteomic Profiling in Yeast, Cell Chemical Biology (2020), https://doi.org/10.1016/j.chembiol.2020.05.006

into transparent glass tubes (VWR), irradiated with 365 nm UV light (Entela, Upland, CA). After a 2 h incubation at 25°C with magnetic stirring, the supernatant was collected, desalted as described above, evaporated to dryness by SpeedVac, and stored at -20°C until LC-MS/MS analysis.

LC-MS/MS Analysis

For protein-level analysis, LC-MS/MS runs were performed on Q Exactive plus (Thermo Fisher Scientific) operated with an Easy-nLC1000 nanoflow LC system (Thermo Fisher Scientific). Samples were reconstituted in 0.1% formic acid and pressure-loaded onto a 2 cm, 150-μm inner diameter microcapillary precolumn packed with C18 (3 μm, 120 Å, SunChrom, USA). The precolumn was connected to a 12 cm, 150-μm-inner diameter microcapillary analytical column packed with C18 (1.9 μm, 120 Å, Dr. Maisch GebH, Germany) and equipped with a homemade electrospray emitter tip. The spray voltage was set to 2.0 kV and the heated capillary temperature to 320°C. LC gradient consisted of 0 min, 7% B; 14 min, 10% B; 51 min, 20% B; 68 min, 30% B; 69-75 min, 95% B (A = water, 0.1% formic acid; B = ACN, 0.1% formic acid) at a flow rate of 600 nL/min. HCD MS/MS spectra were recorded in the data-dependent mode using a Top 20 method. MS1 spectra were measured with a resolution of 70,000, an AGC target of 3e6, a max injection time of 20 ms, and a mass range from m/z 300 to 1400. HCD MS/MS spectra were acquired with a resolution of 17,500, an AGC target of 1e6, a max injection time of 60 ms, a 1.6 m/z isolation window and normalized collision energy of 30. Peptide m/z that triggered MS/MS scans were dynamically excluded from further MS/MS scans for 18 s.

For site-level analysis, LC-MS/MS runs were performed on Q Exactive HF (Thermo Fisher Scientific) operated with an Easy-nLC1000 nanoflow LC system (Thermo Fisher Scientific). Samples were reconstituted in 0.1% formic acid and pressure-loaded onto a 2 cm, 100-μm inner diameter microcapillary precolumn packed with C18 (3 μm, 120 Å, SunChrom, USA). The precolumn was connected to a 30 cm 150-μm inner diameter microcapillary analytical column packed with C18 (1.9 μm, 120 Å, Dr. Maisch GebH, Germany) and equipped with a homemade electrospray emitter tip. The spray voltage was set to 2.0 kV and the heated capillary temperature to 320°C. LC gradient consisted of 0 min, 5% B; 25 min, 12% B; 110 min, 24% B; 140 min, 40% B; 141-150 min, 95% B (A = HPLC-grade water, 0.1% HPLC-grade formic acid; B = HPLC-grade acetonitrile, 0.1% formic acid) at a flow rate of 600 nL/min. HCD MS/MS spectra were recorded in the data-dependent mode using a Top 20 method. MS1 spectra were measured with a resolution of 120,000, an AGC target of 3e6, a max injection time of 80 ms, and a mass range from m/z 300 to 1400. HCD MS/MS spectra were acquired with a resolution of 15,000, an AGC target of 2e4, a max injection time of 20 ms, a 1.6 m/z isolation window and normalized collision energy of 27. Peptide m/z that triggered MS/MS scans were dynamically excluded from further MS/MS scans for 25 s.

Yeast RNA Labeling, Enrichment and Quantitation

RNA-related experiments were performed in the AirClean 600 PCR WorkStation, using nuclease-free reagents. 30 mL yeast cells of OD600 at 1.0 were prepared and labeled as previously described. After APEX2 labeling, cells were washed twice with PBS buffer and resuspended in 300 μL PBS. Cells were then mixed with an equal amount of glass beads (Sigma) and shaken on a ThermoMixer C (Eppendorf) at 2,000 rpm at 4°C for 1 min. Then the cells were frozen in liquid nitrogen for 30-60 s. After thawing, the "shake-freeze" cycle was repeated for 9 times to lyse yeast cells. After cell lysis was completed, the samples were centrifuged at 12,000 rpm at 4°C for 5 min and the supernatant was collected. Yeast total RNA was extracted by TRIzol reagent (Life Technologies) from the supernatant according to manufacturer's instructions, and then treated with DNase I (NEB) at 37°C for 30 min to remove residual DNA. For samples labeled with Alk-Ph and the corresponding control samples, purified RNA was mixed with 0.1 mM azide-$(PEG)_3$-biotin, 2 mM THPTA (Click Chemistry Tools), 0.5 mM copper sulfate pentahydrate (Aladdin), and 5 mM sodium ascorbate (Aladdin) at room temperature for 10 min. This step was omitted in samples labeled with biotin-phenol and the corresponding control samples. All RNA samples were purified by RNA Clean & Concentrator - 100 (Zymo Research).

Biotinylated RNA was enriched by Dynabeads MyOne Streptavidin C1 beads (Invitrogen). Briefly, C1 beads were washed three times with B&W buffer (5 mM Tris-HCl, pH 7.5, 1 M NaCl, 0.5 mM EDTA, 0.1% v/v Tween-20), twice with NaOH solution (0.1 M NaOH and 0.05 M NaCl), and once with 0.1 M NaCl solution at room temperature. C1 beads were then blocked with blocking buffer (1 mg/mL BSA and 1 mg/mL yeast tRNA in B&W buffer) on a shaker at room temperature for 2 h. The beads were washed three times with B&W buffer under vortexing, mixed with biotinylated RNA, and thoroughly mixed by rotating at room temperature for 45 min.

The RNA-loaded beads were washed three times with B&W buffer, twice with PBS supplemented with 4 M urea and 0.1% SDS, and twice with PBS, at room temperature. RNA was collected by treating beads with elution buffer (95% formamide, 10 mM EDTA, 1.5 mM D-biotin) at 50°C for 5 min and then 90°C for 5 min. The samples were put on a magnetic stand and the supernatant was carefully pipetted out. RNA was extracted by TRIzol from the supernatant according to manufacturer's instructions.

Enriched RNA was reversely transcribed into cDNA by ProtoScript® II First Strand cDNA Synthesis Kit (NEB). The cDNA product was mixed with PowerUp™ SYBR™ Green Master Mix (Applied Biosystems) and analyzed with RT-PCR on StepOnePlus™ Real-Time PCR System (Applied Biosystems). Cytoplasmic marker gene *ACT1* was set as the reference. The relative enrichment levels of each gene was calculated as follows: the ΔCt of each gene was first calculated by taking the difference of Ct values between the enriched sample and the input; then the ΔΔCt of each gene was defined as the difference of ΔCt values between labeled samples and control samples omitting the probe, to eliminate non-specific background binding of RNA onto the beads. The ΔΔCt values for each gene was compared with the reference gene, *ACT1*, to derive the relative enrichment level, which was calculated as the ratio of $2^{-\Delta\Delta Ct}$. Primers used for RT-PCR analysis are listed in the Key Resources Table.

Please cite this article in press as: Li et al., A Clickable APEX Probe for Proximity-Dependent Proteomic Profiling in Yeast, Cell Chemical Biology (2020), https://doi.org/10.1016/j.chembiol.2020.05.006

QUANTIFICATION AND STATISTICAL ANALYSIS

Protein Identification and Quantification

Raw data files were searched against *Saccharomyces cerevisiae* Uniprot canonical database (Downloaded on Jul 26, 2018 with 6049 entries). Database search were performed with pFind studio (Version 3.0.11) (Chi et al., 2018). Precursor ion mass and fragmentation tolerance was set as 10 ppm and 20 ppm, respectively. The maximum number of modifications allowed per peptide was three, as was the maximum number of missed cleavages allowed. The minimum peptide length was set to 6 amino acids. For protein-level analysis, mass shifts of +28.0313 Da (dimethylation, Light, N-term/K) was searched as fixed modifications; +15.9949 Da (oxidation, M) and + 57.0214 Da (carbamidomethylation, C) were searched as variable modifications. For site-level analysis, mass shifts of +15.9949 Da (oxidation, M), +57.0214 Da (carbamidomethylation, C), and +372.1797 ($C_{19}H_{24}N_4O_4$, Alk-Ph-derived modification, Light, Y) were all searched as variable modifications. The FDRs were estimated by the program from the number and quality of peptide-spectrum-match (PSM) to the decoy database. The FDRs at spectrum, peptide, and protein level were set to < 1%.

Quantification of heavy to light ratios ($R_{H/L}$) was performed using pQuant as previously described (Liu et al., 2014). pQuant calculates $R_{H/L}$ values based on each identified PSM scan with a 15 ppm-level *m/z* tolerance window. For protein-level analysis, a differential mass shift of 6.0318 Da on dimethylated peptides was used for quantifying PSM $R_{H/L}$ values. For each independent experiment, only proteins identified by two or more distinct peptides with quantified PSM $R_{H/L}$ values were retained for further analysis. In this regard, the $R_{H/L}$ value of each identified protein was calculated as the median of all corresponding PSM $R_{H/L}$ values. For site-level analysis, a differential modification of 6.02 Da on probe-derived modification was used for quantifying PSM $R_{H/L}$ values. For each independent experiment, The $R_{H/L}$ value of each Alk-Ph-modified tyrosine site was calculated as the median of all corresponding PSM $R_{H/L}$ values.

ROC Analysis to Determine the H/L Ratio Cut-Off

The averaged H/L ratios for quantified proteins were calculated from ±APEX2 duplicates or ±probe duplicates. The true positive rate (TPR) and false positive rate (FPR) were calculated as a function of the averaged H/L ratio:

$$\mathrm{TPR} = \frac{\text{Number of true positives above the H/L ratio}}{\text{Total number of proteins above the H/L ratio}}$$

$$\mathrm{FPR} = \frac{\text{Number of false positives above the H/L ratio}}{\text{Total number of proteins above the H/L ratio}}$$

The receiver operating characteristic curve was created by plotting the TPR against the FPR, for determining the cut-offs (Figures S2I and S2J). H/L ratios of 227 and 173 were chosen as the cut-offs for ±APEX2 and ±probe datasets, respectively.